Gutzwiller renormalization group

Nicola Lanatà, Yong-Xin Yao, Xiaoyu Deng, Cai-Zhuang Wang, Kai-Ming Ho, and Gabriel Kotliar

Phys. Rev. B **93**, 045103 — Published 6 January 2016

DOI: 10.1103/PhysRevB.93.045103

Gutzwiller Renormalization Group

Nicola Lanatà,[1] Yong-Xin Yao,[2] Xiaoyu Deng,[3] Cai-Zhuang Wang,[2] Kai-Ming Ho,[2] and Gabriel Kotliar[3]

[1]*Department of Physics and National High Magnetic Field Laboratory, Florida State University, Tallahassee, Florida 32306, USA*

[2]*Ames Laboratory-U.S. DOE and Department of Physics and Astronomy, Iowa State University, Ames, Iowa IA 50011, USA*

[3]*Department of Physics and Astronomy, Rutgers University, Piscataway, New Jersey 08856-8019, USA*

(Dated: December 3, 2015)

We develop a variational scheme called "Gutzwiller renormalization group" (GRG), which enables us to calculate the ground state of Anderson impurity models (AIM) with arbitrary numerical precision. Our method can exploit the low-entanglement property of the ground state of local Hamiltonians in combination with the framework of the Gutzwiller wavefunction, and indicate that the ground state of the AIM has a very simple structure, which can be represented very accurately in terms of a surprisingly small number of variational parameters. We perform benchmark calculations of the single-band AIM that validate our theory and suggest that the GRG might enable us to study complex systems beyond the reach of the other methods presently available and pave the way to interesting generalizations, e.g., to nonequilibrium transport in nanostructures.

PACS numbers: 71.10.-w, 71.27.+a, 71.15.-m

Introduction.— Impurity models are ubiquitous in condensed matter theory. Originally, the AIM was deviced to describe magnetic impurities embedded in metallic hosts and heavy-fermion compound.[1,2] However, the AIM can be applied to describe many other physical systems, such as quantum dots[3–5] and dissipative two-level systems.[6] The importance of impurity models in condensed matter has grown further with the emergence of dynamical mean-field theory (DMFT)[7] and its success in describing strongly correlated materials.[8–11] In fact, within DMFT, solving the many-body lattice problem amounts to solve recursively an auxiliary AIM.

Among the many methodologies developed to solve impurity models, one of the most successful is the numerical renormalization group (NRG),[2,12] which was originally deviced by Wilson to study the Kondo problem, and was based on the idea of "scaling", previously introduced by Anderson. The starting point of the NRG procedure consists in representing the AIM as a one-dimensional semi-infinite tight-binding linear chain with the impurity situated at one of the boundaries. Within this representation, and by using a logarithmic discretization of the density of states corresponding to exponentially decaying hoppings (Wilson chains), the NRG algorithm consists in a truncation scheme that enables to take into account the coupling between the different length scales progressively, starting from near the impurity (high energies) to longer distances (low energies), while retaining a relatively small number of states at each stage.

More recently, the NRG algorithm has been reinterpreted as a variational method within the framework of the "matrix product states".[13,14] From this perspective, the accuracy of NRG can be traced back into the fact that, due to the locality of the interactions within the above mentioned one-dimensional representation of the AIM, the ground state has very low entanglement, and can be consequently accurately represented by a matrix product state with a small bond dimension. Thanks to this interpretation it was also possible to uncover a connection between NRG and the density matrix renormalization group (DMRG) method,[15,16] which can also be formulated as a variational approximation within the framework of the matrix product states.[17] Eventually, these ideas resulted in an entirely new class of methods named "variational renormalization group" (VRG),[18] with broader applications with respect to both NRG and DMRG, encompassing, e.g., systems with dimension higher than 1.

In this work we introduce a variational technique to solve the AIM called "Gutzwiller renormalization group" (GRG), that combines the Gutzwiller variational method[19–21] with some of the above mentioned ideas underlying NRG and the other VRG methods. Similarly to the ordinary Gutzwiller theory, the GRG consists in optimizing variationally a wavefunction represented as a Slater determinant extended over the entire system — which is *infinite* — multiplied by a *local* operator (named "Gutzwiller projector"), which modifies the corresponding electron configurations. However, in GRG the action of the Gutzwiller projector is not limited only to the correlated impurity. In fact, in analogy with the NRG numerical procedure, in GRG the longer length scales are taken into account with arbitrary accuracy by extending progressively the action of the Gutzwiller projector also to a portion of the one-dimensional bath lying nearby the impurity. Thus, the size of the "projected" region is increased until the desired level of precision is reached.

We perform calculations that indicate that the ground state of the AIM can be represented in very good approximation by a GRG wavefunction with the projector acting only over a few sites. Theoretically, this fact demonstrates that the ground state of the AIM can be described very accurately in terms of a surprisingly small number of variational parameters, which constitutes an

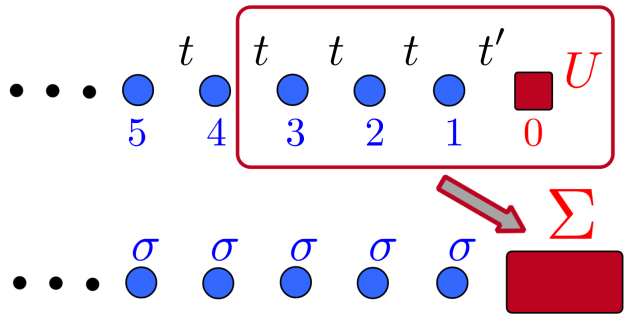

Figure 1: Upper part. Representation of a single-band Anderson impurity model with first nearest neighbor hopping. Each site (bath and impurity) has the elementary spin degree of freedom $\sigma = \pm 1/2$. Lower part. Equivalent representation of the same model where the impurity and a portion of the bath are formally considered as a larger impurity with effective elementary degree of freedom Σ.

interesting general insight about this important system. On the algorithmic side, we show that this fact can be exploited efficiently numerically, and might enable us to solve problems beyond the reach of any other presently available technique.

The Anderson Impurity Model.— For sake of simplicity, here our approach will be formulated for the single-band AIM represented in Fig. 1, where the correlated impurity is connected to a bath constituted by a linear chain with first nearest-neighbor hopping:

$$\hat{H}_{\rm imp} = \frac{U}{2}\Big[1-\sum_{\sigma} c^{\dagger}_{0,\sigma}c_{0,\sigma}\Big]^2 - \sum_{\sigma=\pm\frac{1}{2}} t'\left(c^{\dagger}_{1,\sigma}c_{0,\sigma}+{\rm H.c.}\right) - \sum_{\sigma=\pm\frac{1}{2}}\sum_{R=1}^{\infty} t\left(c^{\dagger}_{R,\sigma}c_{R+1,\sigma}+{\rm H.c.}\right) . \quad (1)$$

The generalization of our theory to generic impurity models is straightforward.

For later convenience, we point out that the hybridization function[2] of $\hat{H}_{\rm imp}$ with respect to the correlated impurity is given by:

$$\lim_{\eta\to 0^+}[\Delta(\omega+i\eta)]_{\sigma\sigma'} = \delta_{\sigma\sigma'}\, g(\omega)\,, \quad (2)$$

where

$$g(\omega) \equiv \begin{cases} \Gamma\left[\frac{\omega}{D} - i\sqrt{1-\left(\frac{\omega}{D}\right)^2}\right] & \text{if } |\omega|\le D \\ \Gamma\left[\frac{\omega}{D} - {\rm sgn}(\omega)\sqrt{1-\left(\frac{\omega}{D}\right)^2}\right] & \text{if } |\omega| > D\,, \end{cases} \quad (3)$$

$D = 2t$, $\Gamma = t'^2/t$, and ${\rm sgn}(\omega)$ is the sign function.

The Method.— In order to illustrate our method, it is convenient to observe that the subsystem of $\hat{H}_{\rm imp}$ consisting of the impurity and the first nearest N bath sites can be equivalently regarded as a larger impurity $\hat{S}_N[\{a^{\dagger}_{\Sigma}, a_{\Sigma}\}]$, where the label $\Sigma = 1, .., 2(N+1)$ runs over the sites $0, .., N$ and the corresponding spins $\sigma = \pm\frac{1}{2}$, see Fig. 1. Within this definition, $\hat{H}_{\rm imp}$ can be schematically represented as follows:

$$\hat{H}_{\rm imp} = \hat{S}_N[\{a^{\dagger}_{\Sigma}, a_{\Sigma}\}] + \sum_{bb'}[B_N]_{bb'}\, b^{\dagger}_b b_{b'} + \sum_{b\Sigma}\left([V^{\dagger}_N]_{b\Sigma}\, b^{\dagger}_b a_{\Sigma} + [V_N]_{\Sigma b}\, a^{\dagger}_{\Sigma} b_b\right) , \quad (4)$$

where the hybridization function Δ_N of $\hat{S}_N$

$$\Delta_N(z) \equiv V_N \frac{1}{z - B_N} V^{\dagger}_N \quad (5)$$

is a well defined $M \times M$ matrix, where $M \equiv 2(N+1)$.

Our approach consists in optimizing variationally a Gutzwiller wavefunction represented as follows:

$$|\Psi_N\rangle \equiv \hat{\mathcal{P}}_N\,|\Psi_0\rangle\,, \quad (6)$$

where $|\Psi_0\rangle$ is the most general Slater determinant, and $\hat{\mathcal{P}}_N$, which is called "Gutzwiller projector", is the most general operator acting within the subsystem $\hat{S}_N$. As in the ordinary Gutzwiller approximation scheme, in order to simplify the task of calculating the expectation value of the Hamiltonian [Eq. (4)], the variational freedom is further restricted by assuming the following conditions:

$$\langle\Psi_0|\,\hat{\mathcal{P}}^{\dagger}_N\hat{\mathcal{P}}_N\,|\Psi_0\rangle = \langle\Psi_0|\Psi_0\rangle = 1 \quad (7)$$

$$\langle\Psi_0|\,\hat{\mathcal{P}}^{\dagger}_N\hat{\mathcal{P}}_N\, a^{\dagger}_{\Sigma}a_{\Sigma'}\,|\Psi_0\rangle = \langle\Psi_0|\, a^{\dagger}_{\Sigma}a_{\Sigma'}\,|\Psi_0\rangle \;\;\forall\;\Sigma,\Sigma'\,, \quad (8)$$

which are called "Gutzwiller constraints". We point out that, while for bulk systems the Gutzwiller variational ansatz is supplemented by the so called "Gutzwiller approximation"[21] (which is exact only in the limit of infinite coordination lattices[22]), for impurity models the method is purely variational, and no further approximation is needed.[23,24]

For $N = 0$ the procedure described above reduces to applying the Gutzwiller projector only onto the correlated impurity — which is the standard Gutzwiller approach for the AIM used, e.g., in Refs. 23,24. In this work, instead, the region of action of the Gutzwiller projector is extended systematically by increasing N until the desired level of accuracy is obtained.

The most evident difficulty to be overcome is that the number of complex independent parameters defining $\hat{\mathcal{P}}_N$ scales as 2^{2M}. In fact, this makes the task of minimizing the total energy with respect to the wavefunction [Eq. (6)] nontrivial already for small N. However, fortunately, this technical problem can be efficiently solved even for relatively large N thanks to the method of Refs. 25–27, which is summarized in the supplemental material for completeness.[28] A remarkable aspect of this numerical scheme is that it enables us to map the above nonlinear constrained minimization into the much simpler task of calculating iteratively the ground state $|\Phi\rangle$ of a finite AIM represented as follows:

$$\hat{H}^{\rm emb}[\mathcal{D},\lambda^c] \equiv \hat{S}_N[\{a^{\dagger}_{\Sigma}, a_{\Sigma}\}]$$

$$+\sum_{s\Sigma=1}^{M}\left(\mathcal{D}_{s\Sigma}\,a_{\Sigma}^{\dagger}f_{s}+\text{H.c.}\right)+\sum_{ss'=1}^{M}\lambda_{ss'}^{c}f_{s'}f_{s}^{\dagger} \quad (9)$$

at half-filling, i.e., within the subspace such that:

$$\left[\sum_{\Sigma=1}^{M}a_{\Sigma}^{\dagger}a_{\Sigma}+\sum_{s=1}^{M}f_{s}^{\dagger}f_{s}\right]|\Phi\rangle=M\,|\Phi\rangle\,. \quad (10)$$

The complex coefficients $\mathcal{D}_{s\Sigma}$ and $\lambda_{ss'}^{c}$ have to be determined numerically following the procedure summarized in the supplemental material.[28] The number of AIM represented as in Eq. (9) to be solved in order to converge scales as $o(M^2)$, and they can be solved independently (in parallel) if necessary.

As shown in the supplemental material, the ground state $|\Phi\rangle$ of $\hat{H}^{\text{emb}}$ for the converged parameters $\mathcal{D}$ and λ^c encodes the expectation value with respect to the corresponding Gutzwiller wavefunction Eq. (6) of any observable $\hat{A}$ in $\hat{S}_N$, i.e.:

$$\langle\Psi_N|\,\hat{A}[\{a_{\Sigma}^{\dagger},a_{\Sigma}\}]\,|\Psi_N\rangle=\langle\Phi|\,\hat{A}[\{a_{\Sigma}^{\dagger},a_{\Sigma}\}]\,|\Phi\rangle\,. \quad (11)$$

For this reason, as in Ref. 26, here we call $\hat{H}^{\text{emb}}$ "embedding Hamiltonian". Concerning the fact that in Eq. (9) the subsystem $\hat{S}_N$ is coupled with a bath of equal dimension, it is interesting to observe that, at least in principle, a Hamiltonian whose bath has the same dimension of the impurity is sufficient to represent *exactly* the impurity ground-state properties of any system (no matter how big it is). This fact can be readily demonstrated making use of the Schmidt decomposition.[29,30]

Let us now discuss how the computational effort to calculate the ground state of $\hat{H}^{\text{emb}}$ scales with M. In order to answer this question it is important to note that $\hat{H}^{\text{emb}}$ is *quadratic* for all degrees of freedom made exception for those corresponding to $\{c_{0,\sigma}^{\dagger},c_{0,\sigma}\}$ within the original representation of the AIM, see Eq. (1). Thanks to this observation, Eq. (9) can be always transformed into a finite one-dimensional chain by tridiagonalization.[2,31] This enables us to calculate $|\Phi\rangle$ using efficient techniques such as DMRG,[13,14] whose computational cost grows only polynomially with M rather than exponentially. Note that in order to perform the specific calculations that we are going to discuss in this work it has not been actually necessary to resort to this stratagem. However, this might be needed in order to study impurity models more complicated than Eq. (1).

We point out that the possibility to incorporate DMRG within our algorithm constitutes a further connection between GRG and the VRG methods mentioned in the introduction (see also Refs. 32,33), as it reflects the fact that our approach can enforce the low-entanglement property of the ground state of local Hamiltonians within the framework of the Gutzwiller wavefunction, and exploit simultaneously both of these ideas.[42]

From the considerations above we deduce that the computational complexity of the GRG algorithm scales polynomially with N, i.e., with the size of the region of action of the Gutzwiller projector. Our remaining task is to understand how big N has to be in order to describe accurately the ground state of the AIM.

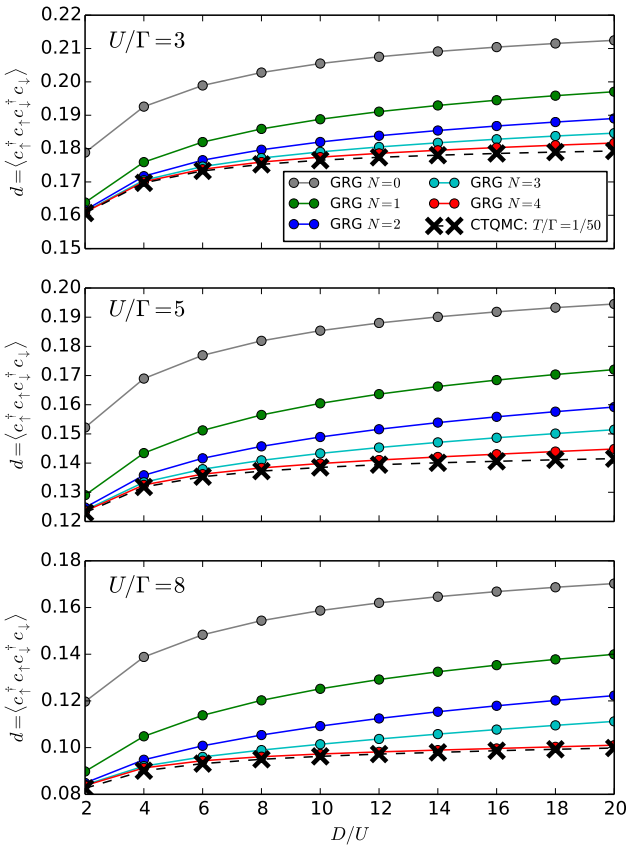

Figure 2: (Color online) Convergence of the GRG expectation value of the double occupancy d with respect to the number of conduction-bath sites N included within the projected region. The result is shown for different U/Γ and D/U in comparison with CTQMC (black crosses).

Benchmark calculations.— In order to assess the quality of the GRG variational ansatz, here we perform benchmark calculations of the single-band AIM at half-filling, see Eq. (1).

In Fig. 2 is shown the behavior of the impurity double occupancy d as a function of D/U for different values of U/Γ. The GRG results obtained with different values of N are shown in comparison with continuous time quantum Monte Carlo (CTQMC)[34,35] as implemented in TRIQS,[36] which were obtained at the temperatures $T/\Gamma=0.02$ and $T/\Gamma=0.01$. From these calculations it emerges that the $N=4$ GRG wavefunction is already sufficient to reproduce very accurately the CTQMC double occupancy for all of the interaction parameters considered. However, we observe that the convergence of d with respect to N becomes increasingly slower for larger D/U, while it is not very sensitive to U/Γ. It is inter-

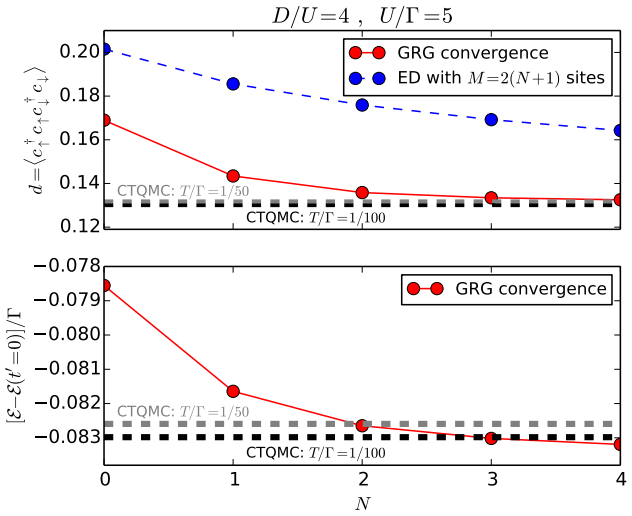

Figure 3: (Color online) Upper panel: Convergence as a function of N of the GRG double occupancy d for $D/U = 4$ and $U/\Gamma = 3$ in comparison with exact diagonalization for the truncated system composed by $2(N + 1)$ sites. Lower panel: Corresponding convergence of the total energy $\mathcal{E}$. The results calculated with CTQMC are indicated by the dotted horizontal lines.

esting to compare this trend with the behavior of the dimension ξ_K of the Kondo cloud. From the Bethe ansatz solution of the single band AIM we know that, in the large-D limit, ξ_K is given by:[2]

$$\xi_K \equiv v_F/T_K \sim \frac{D}{U}\sqrt{\frac{2U}{\Gamma}}e^{\frac{\pi}{8}\frac{U}{\Gamma}+\frac{\pi}{2}\frac{\Gamma}{U}} \qquad (12)$$

(in units of the lattice spacing). As we see from Eq. (12), ξ_K diverges exponentially with U/Γ. Furthermore, we note that ξ_K is much bigger than the value of N necessary to achieve convergence within the GRG. In fact, for instance, substituting the values $D/U = 10$ and $U/\Gamma = 5$ in Eq. (12) we find that $\xi_K \sim 275 \gg 5$. Thus, we deduce that these two length scales are not directly related, as one might naively expect.

In Fig. 3 is shown the behavior of the impurity double occupancy and of the total energy calculated with GRG as a function of the convergence parameter N. Note that the zero of the total energy is conventionally assumed to be the ground state energy of Eq. (1) with $t' = 0$. These data are shown in comparison with CTQMC and with the exact diagonalization results obtained by taking into account only the first $2(N + 1)$ sites of Eq. (1) (and discarding the others).

We observe that both the GRG energy and double occupancy converge very rapidly to their respective exact values. In particular, from the convergence of the total energy we deduce that the GRG describes the ground state of the AIM at all length scales, and not only the the impurity degrees of freedom. Note that this is possible because in our approach the Slater determinant $|\Psi_0\rangle$, which acts over the entire system, is optimized variationally simultaneously with the Gutzwiller projector.[28]

From the comparison between GRG and exact diagonalization it emerges that the dimension of the auxiliary AIM [Eq. (9)] to be solved in order to calculate the GRG solution of any order N is much smaller than the dimension of the truncated AIM that would enable us to solve the problem with comparable precision directly with DMRG.[14] Thus, as discussed before, using DMRG to solve iteratively Eq. (9) within the GRG algorithm seems to be a more convenient option.

Conclusions.— In summary, we have developed a variational method called GRG, that takes advantage simultaneously of two among the most powerful ideas in condensed matter theory: (1) the Gutzwiller wavefunction, that enables us to incorporate the most general single-particle wavefunction (Slater determinant) within the variational space, thus reducing the many-body problem to correcting variationally the corresponding electron configurations with the "Gutzwiller projector"; (2) the VRG methods, that enable us to exploit the low-entanglement property of the ground state of local Hamiltonians. Using the GRG, we have shown that the ground state of the AIM has a very simple structure, which can be represented very accurately in terms of a surprisingly small number of variational parameters. These insights resulted in an efficient algorithm that might enable us to study complex systems beyond the reach of any other method presently available. Another remarkable property of our approach is that it enables us to describe the ground state of the AIM in the thermodynamical limit and at all length scales, while this is technically very difficult with any other existing technique, including NRG, DMRG, and the Bethe ansatz.[37–39] Our work paves the way to several generalizations. In particular, it will be very interesting to generalize it to finite temperatures[40] and to nonequilibrium transport in nanostructures, see Refs. 23,24. In fact, the physics of the AIM out of equilibrium is not still well understood, and different methods seem to produce different results even for simple systems such as the single band AIM.[41]

Acknowledgments

We thank Natan Andrei, Vladimir Dobrosavljević, and Michele Fabrizio for useful discussions. N.L., X.D. and G.K. were supported by U.S. DOE Office of Basic Energy Sciences under Grant No. DE-FG02-99ER45761. Research at Ames Laboratory supported by the U.S. Department of Energy, Office of Basic Energy Sciences, Division of Materials Sciences and Engineering. Ames Laboratory is operated for the U.S. Department of Energy by Iowa State University under Contract No. DE-AC02-07CH11358.

[1] P. W. Anderson, Phys. Rev. **124**, 41 (1961).
[2] A. C. Hewson, *The Kondo Problem to Heavy Fermions* (Cambridge University Press, 1997).
[3] V. Madhavan, W. Chen, T. Jamneala, M. Crommie, and N. S. Wingreen, Science **280**, 567 (1998).
[4] S. M. Cronenwett, T. H. Oosterkamp, and L. P. Kouwenhoven, Science **281**, 540 (1998).
[5] W. G. van der Wiel, S. De Franceschi, J. M. Elzerman, T. Fujisawa, S. Tarucha, and L. P. Kouwenhoven, Rev. Mod. Phys. **75**, 1 (2002).
[6] K. Vladár and A. Zawadowski, Phys. Rev. B **28**, 1564 (1983).
[7] A. Georges, G. Kotliar, W. Krauth, and M. J. Rozenberg, Rev. Mod. Phys. **68**, 13 (1996).
[8] G. Kotliar, S. Y. Savrasov, K. Haule, V. S. Oudovenko, O. Parcollet, and C. A. Marianetti, Rev. Mod. Phys. **78**, 865 (2006).
[9] K. Held, A. Nekrasov, G. Keller, V. Eyert, N. Blümer, A. K. McMahan, R. T. Scalettar, T. Pruschke, V. I. Anisimov, and D. Vollhardt, Phys. Stat. Sol. (B) **243**, 2599 (2006).
[10] T. Maier, M. Jarrell, T. Pruschke, and M. H. Hettler, Rev. Mod. Phys. **77**, 1027 (2005).
[11] V. Anisimov and Y. Izyumov, *Electronic Structure of Strongly Correlated Materials* (Springer, 2010).
[12] K. G. Wilson, Rev. Mod. Phys. **47**, 773 (1975).
[13] H. Saberi, A. Weichselbaum, and J. von Delft, Phys. Rev. B **78**, 035124 (2008).
[14] A. Weichselbaum, F. Verstraete, U. Schollwöck, J. I. Cirac, and J. von Delft, Phys. Rev. B **80**, 165117 (2009).
[15] S. R. White, Phys. Rev. Lett. **69**, 2863 (1992).
[16] S. R. White, Phys. Rev. B **48**, 10345 (1993).
[17] F. Verstraete, D. Porras, and J. I. Cirac, Phys. Rev. Lett. **93**, 227205 (2004).
[18] F. Vaestrate, J. Cirac, and V. Murg, Adv. Phys. **57**, 143 (2008).
[19] M. C. Gutzwiller, Phys. Rev. Lett. **10**, 159 (1963).
[20] M. C. Gutzwiller, Phys. Rev. **134**, A923 (1964).
[21] M. C. Gutzwiller, Phys. Rev. **137**, A1726 (1965).
[22] M. Fabrizio, Phys. Rev. B **76**, 165110 (2007).
[23] N. Lanatà, Phys. Rev. B **82**, 195326 (2010).
[24] N. Lanatà and H. U. R. Strand, Phys. Rev. B **86**, 115310 (2012).
[25] N. Lanatà, P. Barone, and M. Fabrizio, Phys. Rev. B **78**, 155127 (2008).
[26] N. Lanatà, Y.-X. Yao, C.-Z. Wang, K.-M. Ho, and G. Kotliar, Phys. Rev. X **5**, 011008 (2015).
[27] N. Lanatà, Y.-X. Yao, C.-Z. Wang, K.-M. Ho, and G. Kotliar, Unpublished (2015).
[28] Supplemental material: Details about the numerical implementation.
[29] I. Peschel, Braz. J. Phys. **42**, 267 (2012).
[30] G. Knizia and G. K.-L. Chan, Phys. Rev. Lett. **109**, 186404 (2012).
[31] I. Ojalvo and M. Newman, AIAA J. **8**, 1234 (1970).
[32] C.-P. Chou, F. Pollmann, and T.-K. Lee, Phys. Rev. B **86**, 041105 (2012).
[33] O. Sikora, H.-W. Chang, C.-P. Chou, F. Pollmann, and Y.-J. Kao, Phys. Rev. B **91**, 165113 (2015).
[34] A. N. Rubtsov, V. V. Savkin, and A. I. Lichtenstein, Phys. Rev. B **72**, 035122 (2005).
[35] P. Werner, A. Comanac, L. de' Medici, M. Troyer, and A. J. Millis, Phys. Rev. Lett. **97**, 076405 (2006).
[36] O. Parcollet, M. Ferrero, T. Ayral, H. Hafermann, I. Krivenko, L. Messio, and P. Seth (2015), cond-mat/1504.01952.
[37] N. Andrei, Phys. Rev. Lett. **45**, 379 (1980).
[38] N. Andrei, K. Furuya, and J. H. Lowenstein, Rev. Mod. Phys. **55**, 331 (1983).
[39] P. B. Weigmann, JETP Lett. **31**, 364 (1980).
[40] N. Lanatà, X.-Y. Deng, and G. Kotliar, Phys. Rev. B **92**, 081108 (2015).
[41] A. Dirks, S. Schmitt, J. E. Han, F. Anders, P. Werner, and T. Pruschke, Europhys. Lett. **102**, 37011 (2013).
[42] Note that within the framework of Ref. 32 the variational Monte Carlo method was used in order to optimize the state, as it was not technically possible to apply the more efficient DMRG algorithm. Furthermore, the Slater determinant was not optimized variationally, while this is done in our approach.